alternés perpendiculairement à l'axe ternaire avec un chalcogène particulier situé de part et d'autre sur l'axe ternaire terminant ainsi le motif.

Le motif $Mo_{12}X_{14}$ (Fig. 4c) rappelle celui de Mo_9X_{11} avec un plan médian (Mo_3X_3) supplémentaire conduisant à une condensation linéaire de trois clusters Mo_6 suivant l'axe ternaire.

Le nouveau composé $Tl_2Mo_6Se_6$ ne présente que des plans (Mo_3X_3). Il n'existe plus les deux chalcogènes particuliers situés sur l'axe ternaire. Ces deux chalcogènes donnent, dans les autres composés, des motifs finis Mo_6X_8 ($2Mo_3X_3,X_2$), Mo_9X_{11} ($3Mo_3X_3,X_2$) et $Mo_{12}X_{14}$ ($4Mo_3X_3,X_2$). En effet, la présence de ces deux éléments particuliers crée aux extrémités des motifs six faces carrées d'atomes de chalcogène en biseau par rapport à l'axe ternaire qui permettent d'empiler chaque motif avec six motifs voisins, et d'avoir ainsi un recouvrement des orbitales d'un molybdène extrême à un autre molybdène extrême d'un autre motif. Ce recouvrement conduit dans ces phases à une liaison Mo—Mo relativement courte, de l'ordre de 3,10 à 3,50 Å. Dans $Tl_2Mo_6Se_6$, les blocs $(Mo_{6/2}Se_{6/2})^1_\infty$ n'ont plus de faces carrées de sélénium, et la plus courte distance Mo—Mo d'un motif à un autre motif est ici de 6,34 Å; il n'y a plus de couplage métallique entre motifs.

La structure de $Tl_2Mo_6Se_6$ est à rapprocher cristallographiquement de celle de l'alliage Mn_5Si_3 dont la formule structurale s'écrit: $Mn^I_4(Mn^{II}_6Si_6)$ (Aronsson, 1960). $Tl_2Mo_6Se_6$ peut être vu comme une structure lacunaire de celle de Mn_5Si_3. Dans cette dernière, la liaison Mn^I—Mn^{II} = 2,96 Å est courte, enlevant à ce composé tout caractère monodimensionnel.

En conclusion, l'originalité de $Tl_2Mo_6Se_6$ réside dans la très grande anisotropie de sa structure. Des études physiques, notamment électriques, sont en cours et devraient confirmer le caractère monodimensionnel remarquable de ce composé.

Références

Aronsson, B. (1960). *Acta Chem. Scand.* **14**, 1414–1418.
Chevrel, R. (1974). Thèse d'Etat, Rennes.
Chevrel, R., Potel, M., Sergent, M., Decroux, M. & Fischer, Ø. (1980). *J. Solid State Chem.* A paraître.
Germain, G., Main, P. & Woolfson, M. M. (1971). *Acta Cryst.* A**27**, 368–376.
Grüttner, A., Yvon, K., Chevrel, R., Potel, M., Sergent, M. & Seeber, B. (1979). *Acta Cryst.* B**35**, 285–292.
Guillevic, J. (1974). Thèse d'Etat, Rennes.
International Tables for X-ray Crystallography (1974). Tome IV. Birmingham: Kynoch Press.
Le Marouille, J. Y. (1972). Thèse 3ème cycle, Rennes.
McCandlish, L. E., Stout, G. H. & Andrews, L. C. (1975). *Acta Cryst.* A**31**, 245–249.
Meulenaer, J. de & Tompa, H. (1965). *Acta Cryst.* **19**, 1014–1018.
Moore, F. H. (1963). *Acta Cryst.* **16**, 1169–1175.
Potel, M., Chevrel, R. & Sergent, M. (1980). *Acta Cryst.* B**36**, 1319–1322.
Potel, M., Chevrel, R., Sergent, M., Decroux, M. & Fischer, Ø. (1979). *C. R. Acad. Sci. Sér. C*, **288**, 429–432.
Prewitt, C. T. (1966). *SFLS-5. A Fortran IV Full-Matrix Crystallographic Least-Squares Program.* Report ORNL-TM-305. Oak Ridge National Laboratory, Tennessee.
Vand, V., Eiland, P. F. & Pepinsky, R. (1957). *Acta Cryst.* **10**, 303–311.

Acta Cryst. (1980). B**36**, 1548–1554

Structural Studies of Stacking Variants in Mg-Base Friauf–Laves Phases

By Y. Komura and K. Tokunaga*

Faculty of Science, Hiroshima University, Higashi-senda-machi, Hiroshima 730, *Japan*

(*Received* 27 *September* 1979; *accepted* 19 *February* 1980)

Abstract

Five stacking variants in Mg-base Friauf–Laves phases have been refined with three-dimensional X-ray diffraction data from single-crystal fragments of $MgZn_2$ (two-layer), $MgNi_2$ (four-layer) and eight-, nine- and ten-layer-type structures in the $MgZn_2$–$MgAg_2$ system. Full-matrix least-squares refinements yielded $R(F)$ values ranging from 0·053 to 0·079 with isotropic thermal parameters. The hexagonal lattice constants for these structures are a = 5·221 (3), c = 8·567 (6) Å for $MgZn_2$; a = 4·824 (2), c = 15·826 (10) Å for $MgNi_2$; a = 5·210 (3), c = 34·40 (2) Å for eight-layer type; a = 5·210 (3), c = 38·70 (2) Å for nine-layer type; a = 5·220 (3), c = 43·00 (3) Å for ten-layer-type structures. The refinements confirm that these structures are

---

* Present address: Daikin Kogyo Co. Ltd., Sakai, Japan.

0567-7408/80/071548-07$01.00

constructed almost ideally by the stacking of fundamental Laves layers. The kinds of coordination polyhedra surrounding each atom are CN16 Friauf polyhedra for Mg atoms and CN12 icosahedra for small atoms. The structures are thought of as chains of fused coordination polyhedra along [001] with a mode of hexagonal or cubic sequences. The refinements showed that only the small atoms in the connecting planes in the hexagonal mode were shifted, the atoms belonging to the cubic mode were not.

Introduction

A considerable amount of effort has been devoted to the study of the crystal structure in Mg-base Friauf–Laves phases. The crystal structures of $MgZn_2$, $MgCu_2$ and $MgNi_2$ were investigated long ago by Friauf (1927*a*,*b*) and Laves & Witte (1935). These structures are typified as *C*14, *C*15 and *C*36 according to the *Strukturberichte* for $MgZn_2$, $MgCu_2$ and $MgNi_2$, respectively. Laves & Witte (1936) and Lieser & Witte (1952) studied the pseudobinary systems of $MgCu_2$–$MgZn_2$, $MgZn_2$–$MgNi_2$, $MgCu_2$–$MgNi_2$, $MgCu_2$–$MgAl_2$, *etc.* and found a close relationship between crystal structure and electron concentration; that is the phase boundaries of *C*14, *C*15 and *C*36 appear at nearly the same values of *e*/*a* for all the systems studied. Witte (1939) investigated alloys lying along a section $MgZn_2$–$MgAg_2$, and found two transitional types of structure which occurred at approximately 8 mol% $MgAg_2$. Komura (1962), Komura, Kishida & Inoue (1967), Komura, Mitarai, Nakatani, Iba & Shimizu (1970), Komura, Nakaue & Mitarai (1972), Komura, Mitarai, Nakaue & Tsujimoto (1972) and Komura & Kitano (1977) reinvestigated the pseudobinary systems of $MgCu_2$–$MgZn_2$, $MgZn_2$–$MgNi_2$, $MgCu_2$–$MgNi_2$, $MgZn_2$–$MgAg_2$ and $MgCu_2$–$MgAl_2$ in detail, and ascertained that the crystal structures of these systems were strongly governed by the electron concentration. In the course of these investigations, several stacking variants were found in addition to the three fundamental structures *C*14, *C*15 and *C*36. These include six-, eight-, nine-, ten-, 16- and 21-layer-type structures in terms of their layer stackings. Kripyakevich & Melnyk (1974) also reported on the crystal structure for the system $MgZn_2$–$MgLi_2$, in which they added a new stacking variant of the 14-layer type. These new stacking variants were listed in order of electron concentration in a previous paper (Komura & Kitano, 1977). Electron-microscope observations of the Mg-base Friauf–Laves phases were carried out for the $MgCu_2$–$MgAl_2$ system. One-dimensional lattice images of the polytypic structures of the two-, four-, six-, nine-, ten- and 16-layer types were presented by Kitano, Komura & Kajiwara (1977).

In a recent paper, Kitano, Komura, Kajiwara & Watanabe (1980) obtained two-dimensional lattice images of two-, four- and nine-layer-type structures and they reported a new type of linear defect which was always accompanied by stacking faults.

The purpose of the present paper is to refine the several stacking variants of the Friauf–Laves phases, especially two-, four-, eight-, nine- and ten-layer-type structures, and to discuss the structural characteristics found in these stacking variants.

Experimental

The specimens refined in this paper are $MgZn_2$ (*C*14), $MgNi_2$ (*C*36) and eight-, nine- and ten-layer-type structures in the $MgZn_2$–$MgAg_2$ system. Alloys were prepared by melting together pure Mg and Zn for $MgZn_2$ and Mg, Zn and Ag for $MgZn_2$–$MgAg_2$ in an argon-filled induction furnace. An alloy of $MgNi_2$ was prepared by melting Mg–50% Ni mother alloy and pure Ni together in an electrical resistance furnace in the presence of flux ($CaCl_2$, BaF_2 and CaF_2 mixture) in order to prevent oxidation. All alloys thus obtained were then annealed at various temperatures between 670 and 970 K in small graphite crucibles placed inside argon-filled sealed silica tubes. Nominal compositions of the specimens of eight-, nine- and ten-layer structures were $MgZn_2$—0·03$MgAg_2$, $MgZn_2$—0·07$MgAg_2$ and $MgZn_2$—0·10$MgAg_2$, respectively. Chemical analysis showed that the compositions of these alloys

Table 1. *Crystal data*

	$MgZn_2$ (two-layer)	$MgNi_2$ (four-layer)	$MgZn_2$–0·03$MgAg_2$ (eight-layer)	$MgZn_2$–0·07$MgAg_2$ (nine-layer)	MZn_2–0·10$MgAg_2$ (ten-layer)
FW/atom	51·69	47·23	52·54	53·67	54·52
a (Å)	5·221 (3)	4·824 (2)	5·210 (3)	5·210 (3)	5·220 (3)
c (Å)	8·567 (6)	15·826 (10)	34·40 (2)	38·70 (2)	43·00 (3)
V (Å^3)	202·240	318·945	808·657	909·739	1014·705
Space group	$P6_3/mmc$	$P6_3/mmc$	$P6_3/mmc$	$R\bar{3}m$	$P6_3/mmc$
Atoms/hexagonal cell	12	24	48	54	60
D_x (Mg m^{-3})	5·09	5·90	5·18	5·29	5·35
F(000)	288·0	544·0	1168·3	1338·8	1508·0
μ(Mo $K\alpha$) (mm^{-1})	24·1	23·2	23·9	23·7	23·5

did not deviate appreciably. After identifying the phases by X-ray powder diffraction, single crystals were obtained by picking out tiny irregular-shape fragments with average radii about 0·05 mm. The presence of stacking faults was checked by taking Laue, oscillation and Weissenberg photographs. No diffuse streaks were observed for the specimens of the present study. The crystal data for the five structures are summarized in Table 1. Intensity data were collected with Mo $K\alpha$ radiation on an automated Rigaku four-circle diffractometer equipped with a graphite monochromator. θ–2θ scans were used, the scan speed was 2° min^{-1}, and the 2θ range was 1·4° plus the $\alpha_1\alpha_2$ angular separation. Background readings were made at the beginning and the end of each scan range. Each independent reflection was measured at three or four different positions in reciprocal space out to $2\theta = 70°$ and an absorption correction was applied to the averaged intensities, assuming spherical shapes of the specimens. An extinction correction was not applied, though a few reflections with very strong intensities were not taken into account in the least-squares refinements.

Structure refinements

The structure of the Friauf–Laves phase and its stacking variants can be described in terms of the stacking sequence of six compound layers, A, A', B, B', C and C', each of which is composed of a kagomé net and three triangular nets (Komura, 1962). Two compound layers A and A' are shown in Fig. 1. B and B' or C and C' layers can be obtained when A and A' are shifted by $\frac{1}{3}$ or $\frac{2}{3}$ along the [$\bar{1}10$] direction of the hexagonal cell. The layer stacking conforms to the spatial requirements of large Mg atoms, that is each layer can only be followed by two particular layers.

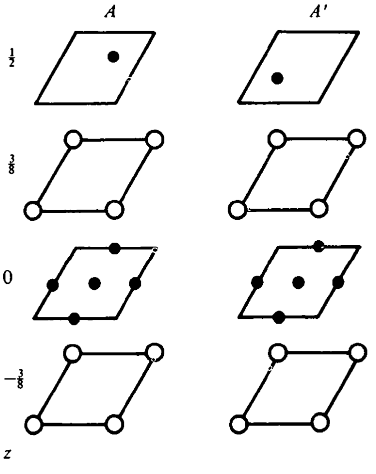

Fig. 1. Two compound layers A and A' of the Friauf–Laves phase. The parameter z is taken as a fraction of the distance between two kagomé nets.

The stacking variants treated in this paper have the following layer sequences (Komura, Mitarai, Nakaue & Tsujimoto, 1972):

layer type	stacking sequence
two-layer ($MgZn_2$)	AB'
four-layer ($MgNi_2$)	$AB'A'C$
eight-layer	$AB'AB'A'CA'C$
nine-layer	$AB'ABC'BCA'C$
ten-layer	$ABC'BCA'C'BC'B'$.

These layer sequences are used as initial structures for the refinements. The refinements were done on a FACOM 230-60 computer at the Kyoto University Computation Centre with *ORFLS* (Busing, Martin & Levy, 1962), modified by Sakurai for the *UNICS* system (1967). The atomic scattering factors listed in *International Tables for X-ray Crystallography* (1962) were employed, with a correction for anomalous dispersion. Zn and Ag atoms were assumed to be distributed at random among the small-atom positions, and weighted average atomic scattering factors were used for the eight-, nine- and ten-layer structures of the $MgZn_2$–$MgAg_2$ system. The agreement factors obtained in the least-squares refinements are listed in Table 2. Scale factors, isotropic temperature factors and atomic positional parameters were refined by full-matrix least squares with special subroutines for the atoms at special positions of different kinds. The final parameters thus obtained are listed in Tables 3, 4, 5 and 6 for the two- and four-, eight-, nine- and ten-layer structures, respectively.*

Table 2. *Agreement factors for the least-squares refinements*

The R factors were calculated by omitting non-observable reflections. Owing to the strong extinction effects a few reflections were omitted in the course of the least-squares refinements.

Specimen	*NO*	Thermal parameters	*NV*	$R(F)$	$R_w(F)$
$MgZn_2$	192	Isotropic	6	0·058	0·061
$MgNi_2$	310	Isotropic	10	0·053	0·061
$MgZn_2$–0·03$MgAg_2$	775	Isotropic	19	0·077	0·074
$MgZn_2$–0·07$MgAg_2$	519	Isotropic	14	0·061	0·059
$MgZn_2$–0·10$MgAg_2$	787	Isotropic	24	0·079	0·081

---

* Lists of structure factors for the five structures have been deposited with the British Library Lending Division as Supplementary Publication No. SUP 35180 (15 pp.). Copies may be obtained through The Executive Secretary, International Union of Crystallography, 5 Abbey Square, Chester CH1 2HU, England.

Table 3. *Final structural parameters for* $MgZn_2$ *and* $MgNi_2$

		x	*y*	*z*	*B* (Å²)
$MgZn_2$					
Mg(1)	4(*f*)	$\frac{1}{3}$	$\frac{2}{3}$	0·06299 (65)	0·90 (8)
Zn(1)	2(*a*)	0	0	0	0·90 (4)
Zn(2)	6(*h*)	−0·16947 (18)	2*x*	$\frac{1}{4}$	0·91 (3)
$MgNi_2$					
Mg(1)	4(*e*)	0	0	0·09400 (38)	0·46 (8)
Mg(2)	4(*f*)	$\frac{1}{3}$	$\frac{2}{3}$	0·84417 (40)	0·58 (9)
Ni(1)	6(*g*)	$\frac{1}{2}$	0	0	0·42 (3)
Ni(2)	6(*h*)	0·16429 (24)	2*x*	$\frac{1}{4}$	0·41 (3)
Ni(3)	4(*f*)	$\frac{1}{3}$	$\frac{2}{3}$	0·12514 (13)	0·37 (3)

Table 4. *Final structural parameters for* $MgZn_2$–0·03$MgAg_2$ (*eight-layer structure*)

*P*6₃/*mmc*		*x*	*y*	*z*	*B* (Å²)
Mg(1)	4(*e*)	0	0	0·04598 (29)	0·67 (14)
Mg(2)	4(*e*)	0	0	0·29611 (28)	0·67 (14)
Mg(3)	4(*f*)	$\frac{1}{3}$	$\frac{2}{3}$	−0·07808 (30)	0·78 (14)
Mg(4)	4(*f*)	$\frac{1}{3}$	$\frac{2}{3}$	−0·17139 (33)	1·08 (16)
Zn,Ag(1)	4(*f*)	$\frac{1}{3}$	$\frac{2}{3}$	0·06235 (11)	1·18 (5)
Zn,Ag(2)	4(*f*)	$\frac{1}{3}$	$\frac{2}{3}$	0·18738 (11)	1·14 (5)
Zn,Ag(3)	6(*g*)	$\frac{1}{2}$	0	0	1·06 (4)
Zn,Ag(4)	6(*h*)	0·50221 (37)	2*x*	$\frac{1}{4}$	1·05 (4)
Zn,Ag(5)	12(*k*)	0·16451 (28)	2*x*	0·12494 (5)	1·28 (3)

Table 5. *Final structural parameters for* $MgZn_2$–0·07$MgAg_2$ (*nine-layer structure*)

Hexagonal axes are adopted for the space group $R\bar{3}m$.

$R\bar{3}m$		*x*	*y*	*z*	*B* (Å²)
Mg(1)	6(*c*)	0	0	0·04171 (18)	0·61 (10)
Mg(2)	6(*c*)	0	0	0·18058 (19)	0·77 (10)
Mg(3)	6(*c*)	0	0	0·26409 (17)	0·47 (9)
Zn,Ag(1)	18(*h*)	0·16391 (17)	$\bar{x}$	0·11111 (3)	0·94 (2)
Zn,Ag(2)	9(*e*)	$\frac{1}{2}$	0	0	1·01 (3)
Zn,Ag(3)	6(*c*)	0	0	0·38870 (6)	0·83 (3)
Zn,Ag(4)	3(*b*)	0	0	$\frac{1}{2}$	0·92 (5)

Table 6. *Final structural parameters for* $MgZn_2$–0·10$MgAg_2$ (*ten-layer structure*)

*P*6₃/*mmc*		*x*	*y*	*z*	*B* (Å²)
Mg(1)	4(*e*)	0	0	0·21220 (37)	0·56 (24)
Mg(2)	4(*f*)	$\frac{1}{3}$	$\frac{2}{3}$	0·11282 (38)	0·73 (25)
Mg(3)	4(*f*)	$\frac{1}{3}$	$\frac{2}{3}$	0·18696 (41)	0·93 (27)
Mg(4)	4(*f*)	$\frac{1}{3}$	$\frac{2}{3}$	0·51306 (40)	0·87 (27)
Mg(5)	4(*f*)	$\frac{1}{3}$	$\frac{2}{3}$	0·58712 (35)	0·45 (23)
Zn,Ag(1)	2(*a*)	0	0	0	1·30 (13)
Zn,Ag(2)	4(*e*)	0	0	0·10003 (14)	1·28 (9)
Zn,Ag(3)	4(*f*)	$\frac{1}{3}$	$\frac{2}{3}$	0·69987 (14)	1·28 (10)
Zn,Ag(4)	6(*h*)	0·49763 (66)	2*x*	$\frac{1}{4}$	1·15 (7)
Zn,Ag(5)	12(*k*)	0·16940 (46)	2*x*	0·05002 (7)	1·15 (5)
Zn,Ag(6)	12(*k*)	0·16661 (47)	2*x*	0·64998 (7)	1·18 (5)

Characteristics of the structure

Results of the least-squares refinements show that the positions of atoms in each structure, except for a few small atoms, are shifted very little from the initial positions which were constructed by assuming the regular stacking of fundamental Laves layers. The few small atoms in each structure were shifted at most by about 3 parts in 1000 in the planes of the kagomé nets. This produced longer and shorter distances in the hexagons of the kagomé nets. The crystal structure of another stacking variant of the six-layer type has already been determined (Komura, Nakaue & Mitarai, 1972). The characteristics of this structure are similar to the above-described structures. No attempt has been made to estimate the atomic ordering and deviation of alloy compositions for the $MgZn_2$–$MgAg_2$ system. The errors due to these effects were thought to be small, since the atomic fractions of Ag are rather small and the weighted average scattering factors were used.

Interatomic distances for the five structures were calculated on the basis of the refined atomic parameters. They are given in Tables 7, 8, 9 and 10. Only distances less than 3·5 Å are included. Coordination polyhedra around Mg atoms and small atoms (Zn, Ni or Ag) form CN16 Friauf polyhedra (Samson, 1958) and CN12 icosahedra, respectively. In Fig. 2 these coordination polyhedra are shown for the structure of $MgZn_2$ projected on the (001) plane. Here the CN16 Friauf polyhedron is shown as a truncated tetrahedron with four atoms out of the planes of the hexagons. The

Table 7. *Interatomic distances* (Å) *for* $MgZn_2$ *and* $MgNi_2$

$MgZn_2$

Mg(1)–Mg(1)	3·204 (8)	Zn(1)–Mg(1) ×6	3·062 (2)
Mg(1) ×3	3·202 (3)	Zn(2) ×6	2·634 (2)
Zn(1) ×3	3·062 (2)		
Zn(2) ×9	3·063 (4)	Zn(2)–Mg(1) ×6	3·063 (4)
		Zn(1) ×2	2·634 (2)
		Zn(2) ×2	2·567 (2)
		Zn(2) ×2	2·654 (2)

$MgNi_2$

Mg(1)–Mg(1)	2·975 (9)	Ni(1)–Mg(1) ×4	2·834 (3)
Mg(2) ×3	2·952 (3)	Mg(2) ×2	2·832 (6)
Ni(1) ×6	2·834 (3)	Ni(1) ×4	2·412 (1)
Ni(2) ×3	2·825 (6)	Ni(3) ×2	2·421 (2)
Ni(3) ×3	2·828 (2)		
		Ni(2)–Mg(1) ×2	2·825 (6)
Mg(2)–Mg(1) ×3	2·952 (3)	Mg(2) ×4	2·835 (4)
Mg(2)	2·981 (9)	Ni(2) ×2	2·378 (2)
Ni(1) ×3	2·832 (6)	Ni(2) ×2	2·446 (2)
Ni(2) ×6	2·835 (4)	Ni(3) ×2	2·429 (2)
Ni(3) ×3	2·827 (2)		
		Ni(3)–Mg(1) ×3	2·828 (2)
		Mg(2) ×3	2·827 (2)
		Ni(1) ×3	2·421 (2)
		Ni(2) ×3	2·429 (2)

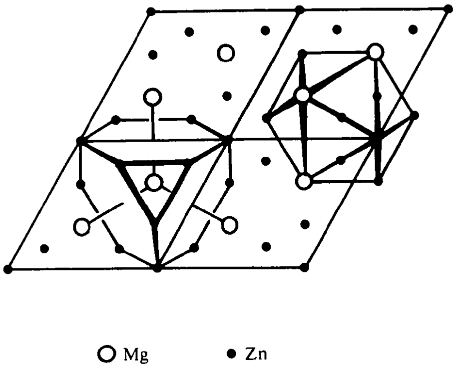

Fig. 2. Projection of the structure of $MgZn_2$ onto the (001) plane. The CN16 Friauf polyhedron and CN12 icosahedron are shown schematically in the figure.

Table 8. *Interatomic distances* (Å) *for* $MgZn_2$–$0{\cdot}03MgAg_2$ (*eight-layer structure*)

Atoms Zn indicate averaged atom sites of Zn, Ag.

Mg(1)–Mg(1)		3·163 (14)
	Mg(3) ×3	3·204 (5)
	Zn(1) ×3	3·060 (3)
	Zn(3) ×6	3·048 (5)
	Zn(5) ×3	3·095 (9)
Mg(2)–Mg(2)		3·172 (14)
	Mg(4) ×3	3·209 (5)
	Zn(2) ×3	3·061 (2)
	Zn(4) ×6	3·050 (6)
	Zn(5) ×3	3·095 (9)
Mg(3)–Mg(1) ×3		3·204 (5)
	Mg(4)	3·210 (15)
	Zn(1) ×3	3·056 (2)
	Zn(3) ×3	3·078 (9)
	Zn(5) ×6	3·063 (6)
Mg(4)–Mg(2) ×3		3·209 (5)
	Mg(3)	3·210 (15)
	Zn(2) ×3	3·058 (3)
	Zn(4) ×3	3·085 (10)
	Zn(5) ×6	3·056 (6)
Zn(1)–Mg(1) ×3		3·060 (3)
	Mg(3) ×3	3·056 (2)
	Zn(3) ×3	2·620 (3)
	Zn(5) ×3	2·638 (4)
Zn(2)–Mg(2) ×3		3·061 (2)
	Mg(4) ×3	3·058 (3)
	Zn(4) ×3	2·639 (4)
	Zn(5) ×3	2·633 (4)
Zn(3)–Mg(1) ×4		3·048 (5)
	Mg(3) ×2	3·078 (9)
	Zn(1) ×2	2·620 (3)
	Zn(3) ×4	2·605 (1)
Zn(4)–Mg(2) ×4		3·050 (6)
	Mg(4) ×2	3·085 (10)
	Zn(2) ×2	2·639 (4)
	Zn(4) ×2	2·570 (4)
	Zn(4) ×2	2·640 (4)
Zn(5)–Mg(1)		3·095 (9)
	Mg(2)	3·095 (9)
	Mg(3) ×2	3·063 (6)
	Mg(4) ×2	3·056 (6)
	Zn(1)	2·638 (4)
	Zn(2)	2·633 (4)
	Zn(5) ×2	2·571 (3)
	Zn(5) ×2	2·639 (3)

Table 9. *Interatomic distances* (Å) *for* $MgZn_2$–$0{\cdot}07MgAg_2$ (*nine-layer structure*)

Atoms Zn indicate averaged atom sites of Zn, Ag.

Mg(1)–Mg(1)		3·288 (10)
	Mg(3) ×3	3·191 (4)
	Zn(1) ×3	3·066 (6)
	Zn(2) ×6	3·065 (4)
	Zn(3) ×3	3·054 (2)
Mg(2)–Mg(2) ×3		3·195 (4)
	Mg(3)	3·232 (10)
	Zn(1) ×3	3·069 (7)
	Zn(1) ×6	3·063 (4)
	Zn(4) ×3	3·056 (2)
Mg(3)–Mg(1) ×3		3·191 (4)
	Mg(2)	3·232 (10)
	Zn(1) ×6	3·068 (4)
	Zn(2) ×3	3·073 (6)
	Zn(3) ×3	3·056 (2)
Zn(1)–Mg(1)		3·066 (6)
	Mg(2)	3·069 (7)
	Mg(2) ×2	3·063 (4)
	Mg(3) ×2	3·068 (4)
	Zn(1) ×2	2·562 (3)
	Zn(1) ×2	2·648 (3)
	Zn(3)	2·644 (2)
	Zn(4)	2·638 (2)
Zn(2)–Mg(1) ×4		3·065 (4)
	Mg(3) ×2	3·073 (6)
	Zn(2) ×4	2·605 (1)
	Zn(3) ×2	2·618 (2)
Zn(3)–Mg(1) ×3		3·054 (2)
	Mg(3) ×3	3·056 (2)
	Zn(1) ×3	2·644 (2)
	Zn(2) ×3	2·618 (2)
Zn(4)–Mg(2) ×6		3·056 (2)
	Zn(1) ×6	2·638 (2)

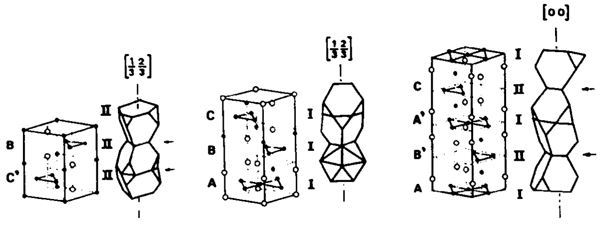

(a) (b) (c)

Fig. 3. The crystal structures and chains of fused coordination polyhedra along [001]. Small arrows indicate atom shifts in the connecting plane of coordination polyhedra. (*a*) $MgZn_2$. (*b*) $MgCu_2$. (*c*) $MgNi_2$.

truncated tetrahedra are arranged so as to make a close-packed layer by sharing three hexagons with three other polyhedra, and thus the Mg atoms form Friauf polyhedra.

There are two ways of connecting Friauf polyhedra when the close-packed layers described above are stacked together. In $MgCu_2$ each Friauf polyhedron of the second layer is turned through 60° with respect to those of the first, whereas in $MgZn_2$ the second Friauf polyhedron is a mirror image of the first one. Samson (1969) called these connections modes I and II, respectively. It is seen that these two modes correspond to the cubic and hexagonal sequences of the compound layers of the Friauf–Laves phases (Komura & Kitano, 1977). Each structure is then thought of as a chain of fused coordination polyhedra along [001] of the hexagonal axis. Fig. 3 shows such chains in the fundamental Laves-phase structures of $MgZn_2$, $MgCu_2$ and $MgNi_2$; here the cubic $MgCu_2$ structure is drawn in terms of hexagonal axes instead of cubic ones. The modes I and II are indicated at the side of the chain of fused coordination polyhedra in Fig. 3. Refinement of the structures shows that only the small atoms in the planes connected in mode II (*i.e.* hexagonal sequence) are shifted inwards or outwards so as to make the Mg–Mg distances longer or shorter. Atoms belonging to mode I are not shifted. In Fig. 4, atom shifts for other structures are indicated by small arrows together with the connecting modes at the right of each chain.

Table 10. *Interatomic distances* (Å) *for* $MgZn_2$–$0{\cdot}10MgAg_2$ (*ten-layer structure*)

Atoms Zn indicate averaged atom sites of Zn, Ag.

Mg(1)—	Mg(1)	3·251 (23)
	Mg(3) ×3	3·203 (8)
	Zn(3) ×3	3·060 (3)
	Zn(4) ×6	3·075 (9)
	Zn(6) ×3	3·070 (14)
Mg(2)—	Mg(3)	3·188 (24)
	Mg(5) ×3	3·210 (8)
	Zn(2) ×3	3·064 (3)
	Zn(5) ×3	3·080 (15)
	Zn(6) ×6	3·060 (9)
Mg(3)—	Mg(1) ×3	3·203 (8)
	Mg(2)	3·188 (24)
	Zn(3) ×3	3·064 (4)
	Zn(4) ×3	3·091 (16)
	Zn(6) ×6	3·056 (10)
Mg(4)—	Mg(4) ×3	3·216 (9)
	Mg(5)	3·185 (23)
	Zn(1) ×3	3·066 (4)
	Zn(5) ×6	3·056 (10)
	Zn(5) ×3	3·091 (16)
Mg(5)—	Mg(2) ×3	3·210 (8)
	Mg(4)	3·185 (23)
	Zn(2) ×3	3·064 (3)
	Zn(5) ×6	3·059 (9)
	Zn(6) ×3	3·095 (14)
Zn(1)—	Mg(4) ×6	3·066 (4)
	Zn(5) ×6	2·640 (4)
Zn(2)—	Mg(2) ×3	3·064 (3)
	Mg(5) ×3	3·064 (3)
	Zn(5) ×3	2·640 (6)
	Zn(6) ×3	2·623 (6)
Zn(3)—	Mg(1) ×3	3·060 (3)
	Mg(3) ×3	3·064 (4)
	Zn(4) ×3	2·642 (6)
	Zn(6) ×3	2·622 (6)
Zn(4)—	Mg(1) ×4	3·075 (9)
	Mg(3) ×2	3·091 (16)
	Zn(3) ×2	2·642 (6)
	Zn(4) ×2	2·573 (7)
	Zn(4) ×2	2·647 (7)
Zn(5)—	Mg(2)	3·080 (15)
	Mg(4) ×2	3·056 (10)
	Mg(4)	3·091 (16)
	Mg(5) ×2	3·059 (9)
	Zn(1)	2·640 (4)
	Zn(2)	2·640 (6)
	Zn(5) ×2	2·567 (5)
	Zn(5) ×2	2·653 (5)
Zn(6)—	Mg(1)	3·070 (14)
	Mg(2) ×2	3·060 (9)
	Mg(3) ×2	3·056 (10)
	Mg(5)	3·095 (14)
	Zn(2)	2·623 (6)
	Zn(3)	2·622 (6)
	Zn(6) ×2	2·609 (5)
	Zn(6) ×2	2·611 (5)

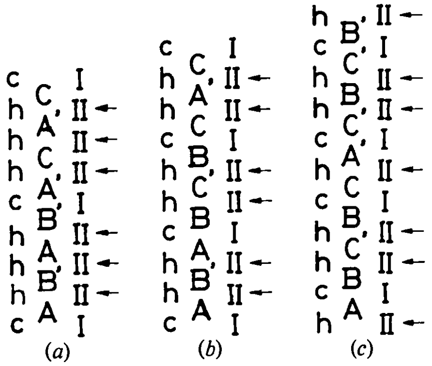

Fig. 4. The stacking sequences and connecting modes of coordination polyhedra. Small arrows indicate atom shifts in the connecting plane of coordination polyhedra. (*a*) Eight-layer type. (*b*) Nine-layer type. (*c*) Ten-layer type.

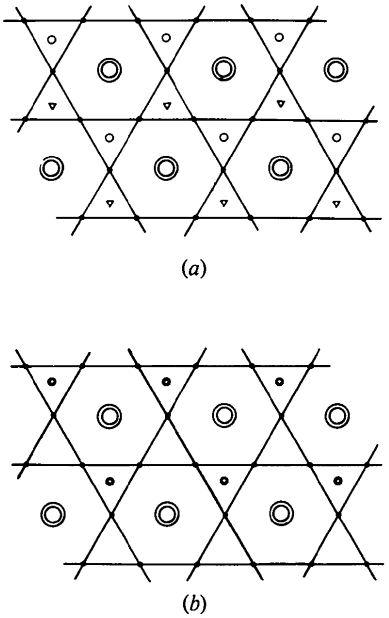

Fig. 5. Atomic arrangements near the kagomé net in the connection modes I and II. ◎ Mg atom in Friauf polyhedron; ● small atom in the kagomé net; ○, ▽ small atoms above and below the kagomé net, respectively. (*a*) Mode I, (*b*) mode II.

For all the two-, four-, six-, eight-, nine- and ten-layer structures, such structural features are the same; that is small atoms situated on the kagomé net connected in mode II are shifted, but the atoms in mode I are not. In mode I, the small atoms above and below the kagomé net are distributed alternately on the small triangles in the kagomé net, while in mode II they are superimposed on the same triangles, as seen in Fig. 5(*a*) and (*b*). The interaction between the small atoms in mode II may act as a force to shift the atoms in the kagomé net a small distance from the regular position, whereas the interactions are balanced in mode I due to the distribution of the small atoms. However, a detailed discussion of the atom shift cannot be made at present.

We wish to thank Mr M. Mitarai of Hiroshima University for his cooperation in part of this work. The authors are also grateful to Professor Y. Saito and Dr S. Sato of the University of Tokyo for allowing us to use the automated counter diffractometer and for giving much valuable assistance during the X-ray intensity measurements. The calculations were carried out on a FACOM 230-60 computer at the Kyoto University Computation Center using the *UNICS* system (1967). The present work has partly been supported by a Scientific Research Grant from the Ministry of Education to which the authors' thanks are due.

References

Busing, W. R., Martin, K. O. & Levy, H. A. (1962). *ORFLS*. Report ORNL-TM-305. Oak Ridge National Laboratory, Oak Ridge, Tennessee.
Friauf, J. B. (1927*a*). *Phys. Rev.* **29**, 35–40.

FRIAUF, J. B. (1927*b*). *J. Am. Chem. Soc.* **49**, 3107–3114.

International Tables for X-ray Crystallography (1962). Vol. III. Birmingham: Kynoch Press.

KITANO, Y., KOMURA, Y. & KAJIWARA, H. (1977). *Trans. Jpn Inst. Met.* **18**, 39–45.

KITANO, Y., KOMURA, Y., KAJIWARA, H. & WATANABE, E. (1980). *Acta Cryst.* A**36**, 16–21.

KOMURA, Y. (1962). *Acta Cryst.* **15**, 770–778.

KOMURA, Y., KISHIDA, E. & INOUE, M. (1967). *J. Phys. Soc. Jpn*, **23**, 398–404.

KOMURA, Y. & KITANO, Y. (1977). *Acta Cryst.* B**33**, 2496–2501.

KOMURA, Y., MITARAI, M., NAKATANI, I., IBA, H. & SHIMIZU, T. (1970). *Acta Cryst.* B**26**, 666–668.

KOMURA, Y., MITARAI, M., NAKAUE, A. & TSUJIMOTO, S. (1972). *Acta Cryst.* B**28**, 976–978.

KOMURA, Y., NAKAUE, A. & MITARAI, M. (1972). *Acta Cryst.* B**28**, 727–732.

KRIPYAKEVICH, P. I. & MELNYK, E. B. (1974). *Metallofizika*, **52**, 71–74.

LAVES, F. & WITTE, H. (1935). *Metallwirtsch. Metallwiss. Metalltech.* **14**, 645–649.

LAVES, F. & WITTE, H. (1936). *Metallwirtsch. Metallwiss. Metalltech.* **15**, 840–842.

LIESER, K. H. & WITTE, H. (1952). *Z. Metallkd.* **43**, 396–401.

SAMSON, S. (1958). *Acta Cryst.* **11**, 851–857.

SAMSON, S. (1969). *Developments in the Structural Chemistry of Alloy Phases*, edited by B. C. GIESSEN, pp. 65–106. New York: Plenum.

UNICS system (1967). *Universal Crystallographic Computation Program System*, edited by T. SAKURAI. Crystallographic Society of Japan.

WITTE, H. (1939). *Z. Angew. Mineral.* **1**, 83–92.

Acta Cryst. (1980). B**36**, 1554–1560

1,2,4-Triazole Complexes. IX.* The Structure of Tris-μ-(4-phenyl-1,2,4-triazole-N^1,N^2)-bis[bis(isothiocyanato)(4-phenyl-1,2,4-triazole-N^1)cobalt(II)] Hydrate, $Co_2(C_8H_7N_3)_5(NCS)_4.xH_2O$ ($x \simeq 2{\cdot}7$)

BY D. W. ENGELFRIET, G. C. VERSCHOOR AND W. DEN BRINKER

Gorlaeus Laboratories, Sections of Coordination Chemistry and X-ray and Electron Diffraction, Leiden State University, PO Box 9502, 2300 *RA Leiden, The Netherlands*

(*Received* 13 *December* 1979; *accepted* 25 *February* 1980)

Abstract

The crystal structure of Co_2(4-phenyl-1,2,4-triazole)$_5(NCS)_4.2{\cdot}7\ H_2O$, $C_{44}H_{35}Co_2N_{19}S_4.2{\cdot}7\ H_2O$, has been determined by single-crystal X-ray diffraction techniques. The compound is orthorhombic, space group *Pbca*, with $a = 16{\cdot}855$ (2), $b = 17{\cdot}841$ (2), $c = 34{\cdot}355$ (4) Å and $Z = 8$, $D_m = 1{\cdot}447$ (4) Mg m^{-3}. Data were collected with a four-circle diffractometer using Mo $K\alpha$ radiation. The structure was solved by Patterson and Fourier techniques and was refined by block-diagonal least squares to a final $R = 0{\cdot}037$ ($R_w = 0{\cdot}045$) for 5089 independent significant reflexions. The compound consists of dimeric units in which two Co^{II} ions are bridged by three phenyltriazole groups. Two N-donating NCS^- groups and a phenyltriazole group coordinating by only one N atom complete the CoN_6 octahedra. The NCS^- groups coordinated to one of the two Co^{II} ions are disordered. Between the dimeric units there are large voids containing solvent molecules.

Introduction

Very recently, a series of compounds was discovered at our laboratory for which chemical analysis yielded the approximate composition $M^{II}(\text{Phetrz})_{2\cdot5}(NCS)_2$ (Haasnoot & Groeneveld, 1980). Here, *M* is a first-row transition metal and Phetrz stands for 4-phenyl-1,2,4-triazole. The stoichiometry of these Phetrz complexes is thus identical to that of $Mn_2(\text{Metrz})_5(NCS)_4$. In a previous paper (Engelfriet, Verschoor & Vermin, 1979), it was shown that the latter compound consists of dimeric units in which two Mn^{II} ions are bridged by three 1,2-coordinating Metrz groups. From the structural formula of Phetrz (Fig. 1), we expected that with this ligand a similar type of compound would be formed.

---

[*] Part VIII: Engelfriet, Groeneveld, Groenendijk, Smit & Nap (1980).

0567-7408/80/071554-07$01.00